

# SCIENTIFIC REPORTS



OPEN

## Differential Membrane Dipolar Orientation Induced by Acute and Chronic Cholesterol Depletion

Received: 3 April 2017

Accepted: 22 May 2017

Published online: 30 June 2017

Parijat Sarkar<sup>1</sup>, Hirak Chakraborty<sup>1,2</sup> & Amitabha Chattopadhyay<sup>1</sup>

Cholesterol plays a crucial role in cell membrane organization, dynamics and function. Depletion of cholesterol represents a popular approach to explore cholesterol-sensitivity of membrane proteins. An emerging body of literature shows that the consequence of membrane cholesterol depletion often depends on the *actual* process (acute or chronic), although the molecular mechanism underlying the difference is not clear. Acute depletion, using cyclodextrin-type carriers, is faster relative to chronic depletion, in which inhibitors of cholesterol biosynthesis are used. With the overall goal of addressing molecular differences underlying these processes, we monitored membrane dipole potential under conditions of acute and chronic cholesterol depletion in CHO-K1 cells, using a voltage-sensitive fluorescent dye in dual wavelength ratiometric mode. Our results show that the observed membrane dipole potential exhibits difference under acute and chronic cholesterol depletion conditions, *even when cholesterol content was identical*. To the best of our knowledge, these results provide, for the first time, molecular insight highlighting differences in dipolar reorganization in these processes. A comprehensive understanding of processes in which membrane cholesterol gets modulated would provide novel insight in its interaction with membrane proteins and receptors, thereby allowing us to understand the role of cholesterol in cellular physiology associated with health and disease.

Biological membranes are complex, non-covalent, highly organized, two-dimensional assemblies of a diverse variety of lipids and proteins that allow confinement of intracellular contents in selective compartments. They impart an identity to individual cells and organelles, besides providing an appropriate environment for proper functioning of membrane proteins. A major representative lipid in higher eukaryotic cellular membranes is cholesterol which is the end product of a long and multistep sterol biosynthetic pathway that parallels sterol evolution<sup>1,2</sup>. Understanding the role of cholesterol is important to gain insight into membrane structure, function, organization and dynamics<sup>3–5</sup>. This is evident from the range of effects it exerts on membranes such as modulation of membrane order, extent of water penetration and membrane thickness<sup>6–9</sup>. Cholesterol is often found distributed nonrandomly in domains or pools in biological and model membranes<sup>3,10–14</sup>. Many of these domains (sometimes termed as ‘lipid rafts’) are believed to be important for the maintenance of membrane structure and function. The idea of such specialized membrane domains assumes significance in cell biology since many physiologically important functions such as membrane sorting and trafficking<sup>15</sup>, signal transduction processes<sup>16</sup>, in addition to the entry of pathogens<sup>17,18</sup> have been attributed to these domains.

Dipole potential is an important electrostatic property of organized molecular assemblies (such as membranes and micelles). The origin of dipole potential is the electrostatic potential difference within the assembly due to the nonrandom arrangement of amphiphile dipoles and solvent (water) molecules at the assembly interface<sup>19–24</sup>. Dipole potential has received relatively less attention in the literature as opposed to transmembrane and zeta potential, and its role in membrane protein function<sup>25</sup> has not been comprehensively addressed. Depending on the orientation of electric dipoles at the membrane interface, the magnitude of dipole potential has been estimated to be 200–1000 mV. Since dipole potential is operative over a relatively small distance within the membrane, the electric field generated due to dipole potential could be very large ( $\sim 10^8$ – $10^9$  Vm<sup>-1</sup>)<sup>20–23</sup>.

In this work, we have explored the possible correlation between cell membrane cholesterol content and membrane dipole potential, under conditions of acute (*e.g.*, by using carriers such as methyl- $\beta$ -cyclodextrin (M $\beta$ CD)) and chronic (metabolic depletion using cholesterol biosynthetic inhibitors) cholesterol depletion. In order to

<sup>1</sup>CSIR-Centre for Cellular and Molecular Biology, Uppal Road, Hyderabad, 500 007, India. <sup>2</sup>School of Chemistry, Sambalpur University, Jyoti Vihar, Burla, Odisha, 768 019, India. Correspondence and requests for materials should be addressed to A.C. (email: [amit@ccmb.res.in](mailto:amit@ccmb.res.in))

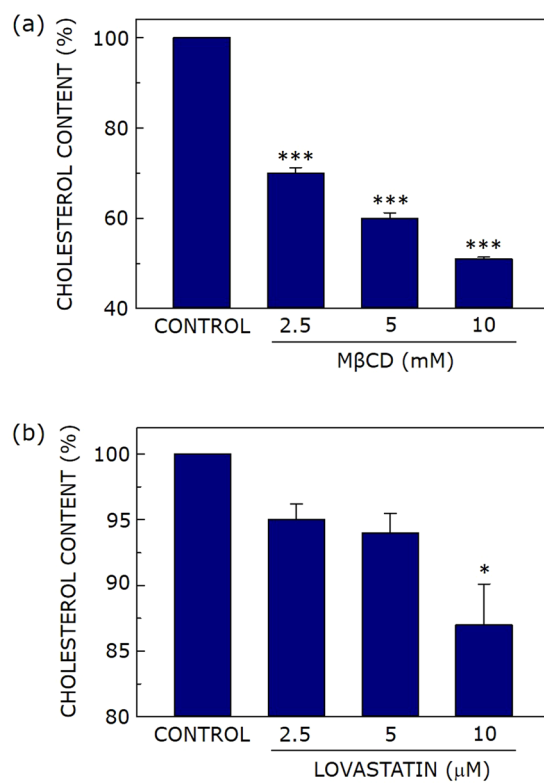


**Figure 1.** Membrane cholesterol depletion upon acute or chronic treatment. Effect of increasing concentration of (a) M $\beta$ CD and (b) lovastatin on cholesterol content of CHO-K1 cell membranes. Values are expressed as percentage of cholesterol content for cell membranes in the absence of M $\beta$ CD or lovastatin treatment. Data represent means  $\pm$  S.E. of at least three independent measurements (\* and \*\*\* correspond to significant ( $p < 0.05$  and  $p < 0.001$ ) difference in cholesterol content of M $\beta$ CD or lovastatin-treated cell membranes relative to untreated membranes). See Methods for other details.

understand the mechanistic framework of membrane organization accompanying modulation of membrane cholesterol, we carried out dipole potential measurements of CHO-K1 cells by a dual wavelength ratiometric imaging approach using an electrochromic probe di-8-ANEPPS<sup>26–30</sup>. Interestingly, membrane cholesterol has been shown to increase dipole potential in model and natural membranes<sup>25, 29, 30</sup> in a stereo-specific manner<sup>31</sup>. In spite of these important structural correlates, the molecular mechanism underlying the modulation of membrane cholesterol is not clear, particularly with reference to the manner in which depletion is carried out (acute *vs.* chronic). We show here, by measurement of membrane dipole potential, that dipolar reorganization could be very different in acute and chronic cholesterol depletion, even when the extent of cholesterol depletion is identical.

## Results

**Concentration-dependent cholesterol depletion from cell membranes by M $\beta$ CD.** Modulation of membrane cholesterol has proved to be an important tool to address cholesterol-dependent function of membrane proteins. For example, we have previously shown that membrane cholesterol is required for the organization and function of the serotonin<sub>1A</sub> receptor, an important member of the G protein-coupled receptor family (GPCR)<sup>32, 33</sup>. This was shown by the depletion of membrane cholesterol either in an acute<sup>34, 35</sup> or chronic<sup>36, 37</sup> manner. Acute cholesterol depletion is achieved by physical depletion of cholesterol using carriers such as M $\beta$ CD, a water soluble carbohydrate polymer that can selectively and efficiently extract cholesterol from membranes by including it in a central nonpolar cavity<sup>38, 39</sup>. Figure 1a shows cholesterol content in membranes of cholesterol-depleted CHO-K1 cells. Upon treatment with increasing concentration of M $\beta$ CD, the cholesterol content of cell membranes shows progressive reduction. For example, cholesterol content was reduced to ~70% of control (without treatment) upon treatment of membranes with 2.5 mM M $\beta$ CD. Maximum (~50%) reduction in cholesterol content was achieved with 10 mM M $\beta$ CD (see Fig. 1a). The concentration range of M $\beta$ CD was carefully chosen to minimize replenishment of membrane cholesterol during the experiment and to avoid loss of phospholipids. The change in phospholipid content under these conditions was negligible, even when 10 mM M $\beta$ CD was used (see Fig. S1).

**Chronic cholesterol depletion upon statin treatment.** Membrane cholesterol depletion using M $\beta$ CD suffers from a number of limitations<sup>38, 40</sup>. A major limitation is that cholesterol depletion using M $\beta$ CD is an acute process due to the relatively short time of treatment. Acute cholesterol depletion therefore may not be a faithful indicator of physiologically relevant cholesterol modulation due to its short time scale. On the other

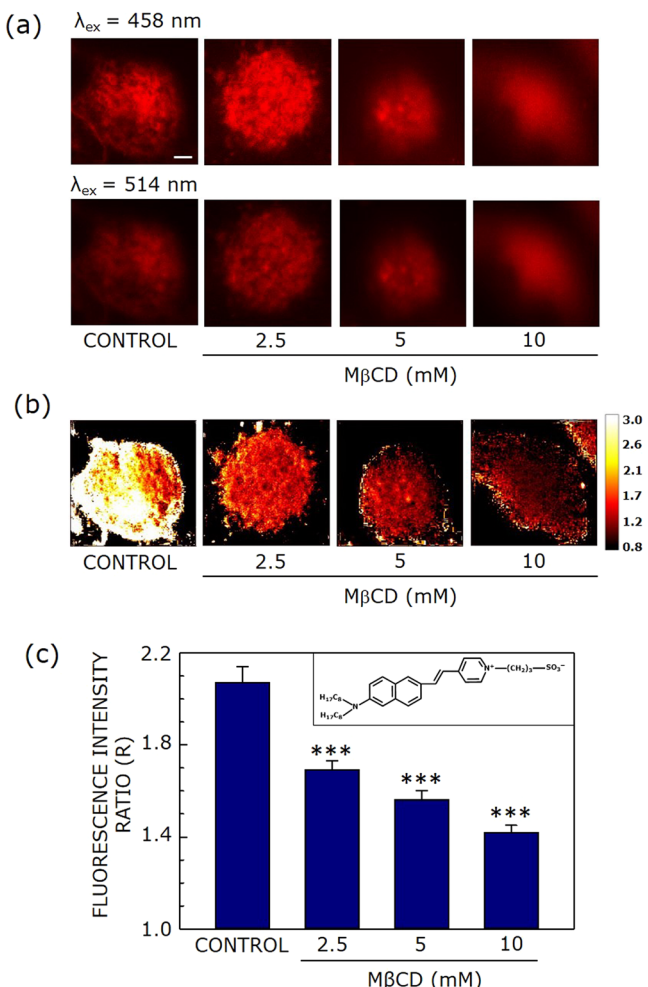


**Figure 2.** Effect of acute cholesterol depletion on membrane dipole potential. **(a)** Representative confocal micrographs of CHO-K1 cells labeled with di-8-ANEPPS ( $\lambda_{ex} = 458 \text{ nm}$  (upper panel), and  $\lambda_{ex} = 514 \text{ nm}$  (lower panel), the emission band pass being 650–710 nm in both cases) with increasing concentrations of M $\beta$ CD. Fluorescence intensity of images was corrected for laser power at two different excitation wavelengths (458 and 514 nm). **(b)** The corresponding fluorescence intensity ratio (R) map (color coded in a scale of 0.8–3) under these conditions. R is defined as the ratio of fluorescence intensities at an excitation wavelength of 458 nm to that at 514 nm (emission band pass at 650–710 nm in both cases) and was calculated using ImageJ (NIH, Bethesda, MD). **(c)** Effect of increasing concentration of M $\beta$ CD on the R value (means  $\pm$  S.E.), averaged over at least fifteen independent measurements (\*\*\* corresponds to significant ( $p < 0.001$ ) difference in R). The scale bar indicates 10  $\mu\text{m}$ . See Methods for more details.

hand, metabolic (chronic) depletion of cholesterol is typically achieved using inhibitors of cholesterol biosynthesis such as statins. Statins are a class of molecules that act as competitive inhibitors of HMG-CoA reductase, the rate-limiting key enzyme in the cholesterol biosynthetic pathway<sup>41,42</sup>. Statins are top selling drugs globally and in clinical history<sup>43</sup>. They are extensively used as oral cholesterol lowering drugs to treat hypercholesterolemia and dyslipidemia<sup>41</sup>. Lovastatin is a commonly used statin which lowers cholesterol content by inhibiting HMG-CoA reductase. Since cholesterol lowering (depletion) by statins takes place over a relatively long period of time, it represents a chronic process, and is physiologically more relevant<sup>37,44</sup>. Figure 1b shows that upon treatment of CHO-K1 cells with increasing concentrations of lovastatin, the cell membrane exhibits progressive reduction in cholesterol content, and ~13% of cholesterol is metabolically depleted when 10  $\mu\text{M}$  lovastatin was used. Control experiments using MTT assay showed that cell viability remained invariant under conditions of acute and chronic cholesterol depletion (data not shown).

**Cholesterol depletion reduces dipole potential of cell membranes.** We utilized the voltage-sensitive fluorescent probe di-8-ANEPPS (see inset in Fig. 2c) for estimating dipole potential of control and cholesterol-depleted cell membranes. The underlying mechanism for the voltage sensitivity of this probe is believed to be electrochromic in nature, leading to a shift of its excitation spectrum, and the shift is proportional to the local electric field strength<sup>45,46</sup>. The advantage of using di-8-ANEPPS is that it undergoes very slow internalization<sup>47</sup>. As a result, the entire fluorescence of di-8-ANEPPS originates from the cell membrane.

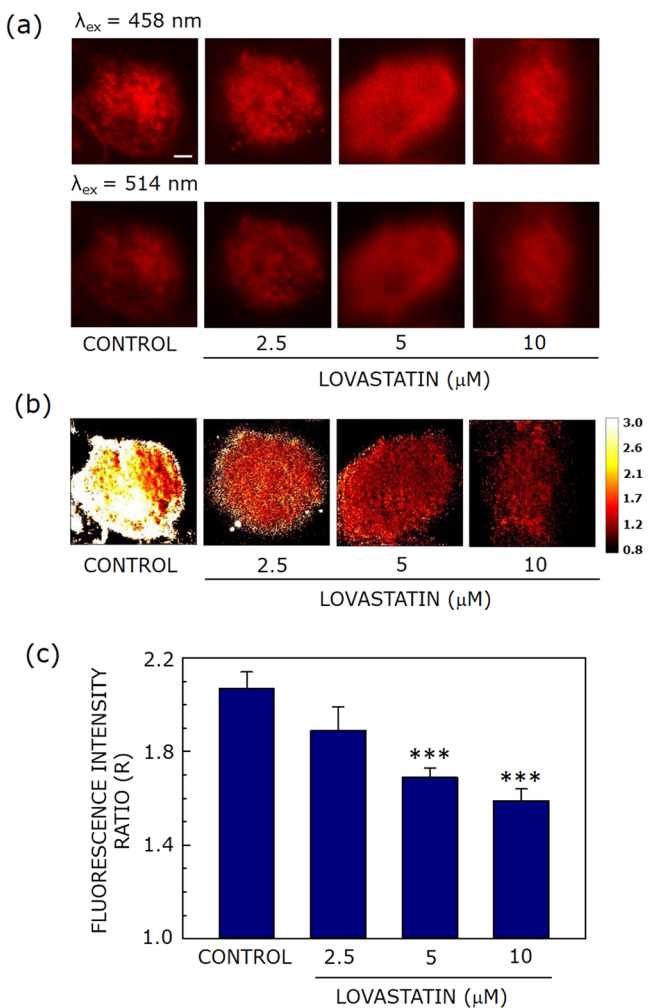


**Figure 3.** Effect of chronic cholesterol depletion on membrane dipole potential. Representative confocal micrographs of CHO-K1 cells labeled with di-8-ANEPPS ( $\lambda_{\text{ex}} = 458 \text{ nm}$  (upper panel), and  $\lambda_{\text{ex}} = 514 \text{ nm}$  (lower panel), the emission band pass being 650–710 nm in both cases) with increasing concentrations of lovastatin. Fluorescence intensity of images was corrected for laser power at two different excitation wavelengths (458 and 514 nm). (b) The corresponding fluorescence intensity ratio (R) map (color coded in a scale of 0.8–3) under these conditions. R is defined as the ratio of fluorescence intensities at an excitation wavelength of 458 nm to that at 514 nm (emission band pass at 650–710 nm in both cases) and was calculated using ImageJ (NIH, Bethesda, MD). (c) Effect of increasing lovastatin concentration on the R value (means  $\pm$  S.E.), averaged over at least fifteen independent measurements (\*\*\* corresponds to significant ( $p < 0.001$ ) difference in R). The scale bar indicates 10  $\mu\text{m}$ . See Methods for more details.

Figures 2a and 3a show representative confocal micrographs of di-8-ANEPPS-labeled CHO-K1 cells using two excitation wavelengths (458 and 514 nm, upper and lower panels, respectively) and emission collected using a 650–710 nm band pass (for both excitation wavelengths), with increasing concentrations of M $\beta$ CD or lovastatin, respectively. The useful parameter in this method of dipole potential measurement is the fluorescence ratio (R) which is the ratio of fluorescence intensities at two different excitation wavelengths with emission wavelength being fixed at the same wavelength. This ratio is sensitive to any change in the dipolar field where the potential-sensitive probe di-8-ANEPPS is localized, and is independent of specific molecular interactions<sup>26,48</sup>. Figure 2b shows a representative map of R (calculated from the ratio of fluorescence intensities from two panels in Fig. 2a) of CHO-K1 cell membranes under conditions of acute cholesterol depletion using increasing concentration of M $\beta$ CD. Figure 2b shows that there is progressive reduction in R with increasing M $\beta$ CD concentration, *i.e.*, with decreasing membrane cholesterol. To obtain a quantitative estimate of R, averaged over a large number of cells, we plotted R (averaged over fifteen different fields) with increasing M $\beta$ CD concentration (see Fig. 2c). The figure shows progressive decrease in R with increasing cholesterol depletion, in overall agreement with Fig. 2b. This is in agreement with previous work by us<sup>25,30</sup> and others<sup>29</sup> where cholesterol was shown to increase dipole potential in membranes. Figure 2c shows ~33% reduction in R in cell membranes treated with 10 mM M $\beta$ CD (corresponding to a ~50% reduction in membrane cholesterol, see Fig. 1a).

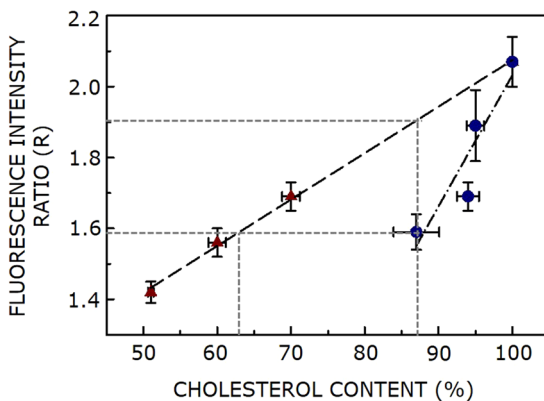


**Figure 4.** Differential dependence of membrane dipole potential on membrane cholesterol content under acute and chronic depletion conditions. A plot of R (a measure of membrane dipole potential, values taken from Figs 2c and 3c) with membrane cholesterol content for acute ( $M\beta$ CD; maroon triangle) and chronic (lovastatin; blue circle) depletion of cholesterol. The cholesterol content data is from Fig. 1. Data points represent means  $\pm$  S.E. and the lines shown are linear fits. An interesting feature is the difference in slope observed under acute ( $\sim 0.013$ ) and chronic ( $\sim 0.037$ ) depletion conditions, thereby indicating a stronger dependence of R on cholesterol content under chronic depletion condition. The orthogonal projections on the axes show that *membrane dipole potential could vary appreciably even when membrane cholesterol content is identical*. See text for more details.

Figure 3 shows the corresponding change in dipole potential (R) under conditions of chronic cholesterol depletion using lovastatin. The change in R upon chronic depletion (with increasing concentration of lovastatin) is shown in Fig. 3b (in a chosen field) and Fig. 3c (averaged over fifteen fields). The decrease in R under these conditions was  $\sim 24\%$  relative to control membranes. Interestingly, we observed that the change in membrane dipole potential upon cholesterol depletion was reversed upon replenishment with cholesterol (see Figs S2 and S3).

**Differential membrane organization revealed by change in dipole potential under acute and chronic cholesterol depletion.** Work from a number of laboratories have demonstrated the crucial role of membrane cholesterol in the function of membrane proteins and receptors<sup>32, 33, 49–55</sup>. However, the detailed mechanism underlying the effect of membrane cholesterol on the structure and function of membrane proteins appears complex<sup>56, 57</sup>. A popular approach to explore cholesterol-sensitivity of membrane proteins has been depletion of membrane cholesterol, followed by monitoring membrane protein function. As mentioned above, this can be achieved by acute<sup>34, 35, 58–63</sup> or chronic<sup>36, 37, 44, 63–65</sup> depletion of membrane cholesterol. Interestingly, the consequences of acute and chronic cholesterol depletion are often different<sup>66–72</sup> and this has resulted in a discussion on the molecular mechanism underlying these processes. For example, these two processes (acute and chronic depletion) have very different consequences on the organization of GPI-anchored proteins and caveole<sup>66</sup>, activity of Na $_+$ -Pi cotransporter<sup>69</sup>, and induction of autophagy<sup>71</sup>. In addition, membrane dynamics (lateral diffusion) appears to be differentially modulated, depending on the actual process of cholesterol depletion<sup>67, 68, 70</sup>. We have previously shown that the function<sup>34, 37</sup> and oligomerization<sup>72</sup> of GPCRs such as the serotonin<sub>1A</sub> receptor exhibit differential response to the actual process of cholesterol modulation.

A closer inspection reveals that the process of cholesterol depletion by agents such as  $M\beta$ CD differs significantly from chronic cholesterol depletion using cholesterol biosynthetic inhibitors such as lovastatin. A hallmark of membrane cholesterol is its nonrandom distribution in domains (or pools) in biological and model membranes<sup>13, 14, 73, 74</sup>. Cholesterol depletion using carriers such as  $M\beta$ CD is known to be a multiphasic process, characterized by differential efficiency of extracting cholesterol from various membrane domains<sup>38, 75, 76</sup>. There appears to be little consensus regarding (differential) extraction efficiency of agents such as  $M\beta$ CD in relation to domain organization of membrane cholesterol and specific experimental conditions used play an important role<sup>39, 66, 76–78</sup>. Although it has been recently reported that acute cholesterol depletion results in loss of cholesterol preferentially from liquid-disordered regions in model membranes<sup>77, 78</sup>, this does not appear to be true in the complex and heterogeneous cellular environment where  $M\beta$ CD does not appear to extract cholesterol preferentially from any specific type of membrane fraction (domain)<sup>79</sup>. On the other hand, chronic cholesterol depletion using biosynthetic inhibitors of cholesterol works in a completely different manner by simply reducing the cellular production of cholesterol, prior to cholesterol localization in various membrane domains. However, chronic cholesterol depletion is complicated by the fact that the effects could be pleiotropic in nature<sup>80</sup> and could even induce cell cycle arrest<sup>81</sup>. In the backdrop of this overall scenario, we addressed fundamental molecular level difference between these two processes by measurement of membrane dipole potential.

In order to gain insight into cholesterol-dependent changes in terms of membrane dipole potential, we plotted R (a measure of dipole potential, from Figs 2c and 3c) as a function of membrane cholesterol content following cholesterol depletion under these conditions (from Fig. 1). This plot is shown in Fig. 4. The figure shows that R drops linearly with decreasing membrane cholesterol content in both cases. A striking feature is the difference in slope observed under acute ( $\sim 0.013$ ) and chronic ( $\sim 0.037$ ) depletion conditions, with  $\sim 2$ -fold higher slope when

cholesterol was depleted in a chronic fashion. This indicates stronger dependence of R on cholesterol content under chronic depletion condition, implying thereby that there is an intrinsic difference between these two processes. When highest concentration ( $10\mu M$ ) of lovastatin was used, ~87% of cholesterol was retained, corresponding to R of ~1.6. A careful inspection of the figure shows that at identical R, ~63% cholesterol remained when depletion was carried out in an acute manner. While it has been previously reported that increasing membrane cholesterol results in higher membrane dipole potential<sup>25, 29, 30</sup>, our present work shows that membrane dipole potential could depend on the actual process used to deplete cholesterol, and not on absolute cholesterol content in the membrane. To the best of our knowledge, these results provide, for the first time, difference between acute and chronic cholesterol depletion at the molecular level in terms of membrane dipolar reorientation.

## Discussion

A fundamental difference between chronic and acute cholesterol depletion is the kinetics of the process. Chronic depletion is a relatively slow process and therefore there is enough time for membrane reorganization, even allowing some of the slowest steps to take place. This will have an effect on membrane dipole potential. Acute depletion, on the other hand, is a faster process and membrane reorganization may not be complete under these conditions. The fact that results from acute cholesterol depletion varies tremendously with experimental conditions (time of treatment, concentration of M $\beta$ CD and cell type)<sup>38</sup> further supports this proposition.

Work from a number of groups has shown that membrane dipole potential is a sensitive indicator of the nature of membrane lipid<sup>29–31, 82</sup>, the function of membrane proteins and peptides<sup>25, 28, 83–85</sup> and in monitoring lipid-protein interaction<sup>86, 87</sup>. Interestingly, we recently introduced the concept of membrane dipole potential in case of organized molecular assemblies such as micelles and showed that micellar dipole potential is a reliable indicator of the process of micellization and shape transition<sup>24, 88</sup>. In this work, we provide a simple and straightforward method to measure dipole potential of cell membranes using commercially available fluorescence confocal microscopic set-up. Our results show that membrane dipole potential, in addition to be dependent on membrane cholesterol content, could reveal interesting difference in dipolar reorientation of membrane components (possibly due to differential membrane reorganization) induced by acute and chronic cholesterol depletion. We believe that these results provide novel insight at a molecular level in the complex interplay between cholesterol and membrane proteins which gets manifested in a variety of biological phenomena. In addition, this could be useful in future drug design since statins represent the best selling drugs in clinical history<sup>43, 89</sup>.

## Methods

**Materials.** 1,2-dimyristoyl-*sn*-glycero-3-phosphocholine (DMPC), CaCl<sub>2</sub>, EDTA, gentamycin sulfate, M $\beta$ CD, 3-(4,5-dimethylthiazol-2-yl)-2,5-diphenyl-tetrazolium bromide (MTT), MgCl<sub>2</sub>, Na<sub>2</sub>HPO<sub>4</sub>, penicillin, phenylmethylsulfonyl fluoride (PMSF), sodium bicarbonate, streptomycin, and Tris were obtained from Sigma Chemical Co. (St. Louis, MO). DMEM/F-12 [Dulbecco's modified Eagle's medium/nutrient mixture F-12 (Ham) (1:1)] and fetal calf serum (FCS) were from Gibco/Life Technologies (Grand Island, NY). Bicinchoninic acid (BCA) reagent for protein estimation was from Pierce (Rockford, IL). Lovastatin was obtained from Calbiochem (San Diego, CA). 4-(2-(6-(Diethylamino)-2-naphthalenyl)ethenyl)-1-(3-sulfopropyl)-pyridinium inner salt (di-8-ANEPPS) was purchased from Molecular Probes (Eugene, OR). The concentration of stock solution of di-8-ANEPPS in methanol was estimated from its molar extinction coefficient ( $\varepsilon$ ) of  $37,000\text{ M}^{-1}\text{cm}^{-1}$  at  $498\text{ nm}$ <sup>46</sup>. All other chemicals used were of the highest available purity. Water was purified through a Millipore (Bedford, MA) Milli-Q system and used throughout.

**Cell culture and cholesterol modulation of cells in culture.** Chinese Hamster Ovary (CHO-K1) cells were maintained in DMEM/F-12 (1:1) supplemented with  $2.4\text{ g/l}$  sodium bicarbonate, 10% FCS, and  $60\mu\text{g/ml}$  penicillin,  $50\mu\text{g/ml}$  streptomycin,  $50\mu\text{g/ml}$  gentamycin sulfate (complete DMEM) in a humidified atmosphere with 5% CO<sub>2</sub> at  $37^\circ\text{C}$ . Stock solution of lovastatin was prepared as described previously<sup>90</sup>. Cells were grown for 24 h in complete DMEM and then treated with increasing concentration of lovastatin for 48 h in complete DMEM. Control cells were grown under similar conditions in the absence of lovastatin. Acute cholesterol depletion was carried out using M $\beta$ CD as described previously<sup>34</sup>. Briefly, cells were grown for 3 days followed by incubation in serum-free DMEM for 3 h at  $37^\circ\text{C}$ . Cholesterol depletion was carried out by treating cells with increasing concentration of M $\beta$ CD in serum-free DMEM for 30 min at  $37^\circ\text{C}$ , followed by washing with PBS, pH 7.4 buffer. Replenishment of cholesterol to M $\beta$ CD or lovastatin-treated cells was carried out as described previously<sup>81</sup>.

**MTT viability assay.** Viability of cells upon cholesterol depletion was assessed using MTT assay as described earlier<sup>91</sup>.

**Cell membrane preparation.** Cell membranes were prepared as described previously<sup>92</sup>. Briefly, confluent cells were harvested by treatment with ice-cold buffer containing 10 mM Tris, 5 mM EDTA, 0.1 mM PMSF, pH 7.4. Cells were then homogenized for 10 s at  $4^\circ\text{C}$  at maximum speed with a Polytron homogenizer. The cell lysate was centrifuged at  $500 \times g$  for 10 min at  $4^\circ\text{C}$  and the resulting post-nuclear supernatant was centrifuged at  $40,000 \times g$  for 30 min at  $4^\circ\text{C}$ . The pellet obtained was suspended in 50 mM Tris buffer, pH 7.4, flash frozen in liquid nitrogen and stored at  $-80^\circ\text{C}$  till further use. The total protein concentration in the isolated membranes was determined using BCA assay<sup>93</sup>.

**Estimation of cholesterol and phospholipid contents.** Cholesterol content in cell membranes was estimated using Amplex Red cholesterol assay kit<sup>94</sup>. Total phospholipid content of membranes was determined subsequent to digestion with perchloric acid using Na<sub>2</sub>HPO<sub>4</sub> as standard<sup>95</sup>. DMPC was used as an internal standard to assess lipid digestion. Samples without perchloric acid digestion produced negligible readings.

**Di-8-ANEPPS labeling of CHO-K1 cells.** Membrane dipole potential measurements were carried out by dual wavelength ratiometric approach using voltage sensitive fluorescence probe di-8-ANEPPS<sup>26–30</sup>. Briefly, cells were plated at a density of ~10<sup>4</sup> on glass cover slips and grown in complete DMEM. Following lovastatin or MβCD treatment, cells were washed with PBS and stained with 1 μM di-8-ANEPPS in serum-free DMEM for 30 min at 4 °C. Cells were then washed, fixed with 3.5% (v/v) formaldehyde for 10 min and mounted.

**Ratiometric fluorescence imaging.** All images were acquired on an inverted Zeiss LSM 510 Meta confocal microscope (Jena, Germany) with a 63×/1.4 NA oil immersion objective under 1 airy condition. Di-8-ANEPPS labeled CHO-K1 cells were imaged using two excitation wavelengths (458 and 514 nm, corresponding to Argon laser lines) with a 650–710 nm emission band pass. The choice of the emission wavelength at the red edge of the fluorescence spectrum has previously been shown to rule out membrane fluidity effects<sup>27</sup>. Fluorescence intensity of images was corrected for the laser power at two different excitation wavelengths (458 and 514 nm). The fluorescence intensity ratio (R), defined as the ratio of fluorescence intensities at an excitation wavelength of 458 nm to that at 514 nm (650–710 nm emission band pass in both cases) was calculated using ImageJ (NIH, Bethesda, MD). A background intensity image was subtracted from the data for each image.

**Statistical analysis.** Significance levels were estimated using Student's two-tailed unpaired *t*-test using Graphpad Prism version 4.0 (San Diego, CA). The correlation between fluorescence intensity ratio and membrane cholesterol content was analyzed using the same software. Plots were generated using Microcal Origin version 6.0 (OriginLab, Northampton, MA).

## References

- Bloch, K. E. Sterol structure and membrane function. *Crit. Rev. Biochem. Mol. Biol.* **14**, 47–92 (1983).
- Nes, W. D. Biosynthesis of cholesterol and other sterols. *Chem. Rev.* **111**, 6423–6451 (2011).
- Simons, K. & Ikonen, E. How cells handle cholesterol. *Science* **290**, 1721–1726 (2000).
- Mouritsen, O. G. & Zuckermann, M. J. What's so special about cholesterol? *Lipids* **39**, 1101–1113 (2004).
- Krause, M. R. & Regen, S. L. The structural role of cholesterol in cell membranes: from condensed bilayers to lipid rafts. *Acc. Chem. Res.* **47**, 3512–3521 (2014).
- Arora, A., Raghuraman, H. & Chattopadhyay, A. Influence of cholesterol and ergosterol on membrane dynamics: a fluorescence approach. *Biochem. Biophys. Res. Commun.* **318**, 920–926 (2004).
- Subczynski, W. K., Wisniewska, A., Yin, J.-J., Hyde, J. S. & Kusumi, A. Hydrophobic barriers of lipid bilayer membranes formed by reduction of water penetration by alkyl chain unsaturation and cholesterol. *Biochemistry* **33**, 7670–7681 (1994).
- Parasassi, T., Di Stefano, M., Loiero, M., Ravagnan, G. & Gratton, E. Cholesterol modifies water concentration and dynamics in phospholipid bilayers: a fluorescence study using Laurdan probe. *Biophys. J.* **66**, 763–768 (1994).
- Nezil, F. A. & Bloom, M. Combined influence of cholesterol and synthetic amphiphilic peptides upon bilayer thickness in model membranes. *Biophys. J.* **61**, 1176–1183 (1992).
- Liscum, L. & Underwood, K. W. Intracellular cholesterol transport and compartmentation. *J. Biol. Chem.* **270**, 15443–15446 (1995).
- Schroeder, F., Woodford, J. K., Kavecansky, J., Wood, W. G. & Joiner, C. Cholesterol domains in biological membranes. *Mol. Membr. Biol.* **12**, 113–119 (1995).
- Simons, K. & Ikonen, E. Functional rafts in cell membranes. *Nature* **387**, 569–572 (1997).
- Xu, X. & London, E. The effect of sterol structure on membrane lipid domains reveals how cholesterol can induce lipid domain formation. *Biochemistry* **39**, 843–849 (2000).
- Chaudhuri, A. & Chattopadhyay, A. Transbilayer organization of membrane cholesterol at low concentrations: implications in health and disease. *Biochim. Biophys. Acta* **1808**, 19–25 (2011).
- Simons, K. & van Meer, G. Lipid sorting in epithelial cells. *Biochemistry* **27**, 6197–6202 (1988).
- Simons, K. & Toomre, D. Lipid rafts and signal transduction. *Nat. Rev. Mol. Cell Biol.* **1**, 31–39 (2000).
- Pucadyil, T. J. & Chattopadhyay, A. Cholesterol: a potential therapeutic target in *Leishmania* infection? *Trends Parasitol.* **23**, 49–53 (2007).
- Kumar, G. A., Jafurulla, M. & Chattopadhyay, A. The membrane as the gatekeeper of infection: cholesterol in host-pathogen interaction. *Chem. Phys. Lipids* **199**, 179–185 (2016).
- Brockman, H. Dipole potential of lipid membranes. *Chem. Phys. Lipids* **73**, 57–79 (1994).
- Clarke, R. J. The dipole potential of phospholipid membranes and methods for its detection. *Adv. Colloid Interface Sci.* **89–90**, 263–281 (2001).
- O'Shea, P. Physical landscapes in biological membranes: physico-chemical terrains for spatio-temporal control of biomolecular interactions and behaviour. *Philos. Trans. A. Math. Phys. Eng. Sci.* **363**, 575–588 (2005).
- Wang, L. Measurements and implications of the membrane dipole potential. *Annu. Rev. Biochem.* **81**, 615–635 (2012).
- Jewell, S. A., Petrov, P. G. & Winlove, C. P. The effect of oxidative stress on the membrane dipole potential of human red blood cells. *Biochim. Biophys. Acta* **1828**, 1250–1258 (2013).
- Sarkar, P. & Chattopadhyay, A. Dipolar rearrangement during micellization explored using a potential-sensitive fluorescent probe. *Chem. Phys. Lipids* **191**, 91–95 (2015).
- Singh, P., Halder, S. & Chattopadhyay, A. Differential effect of sterols on dipole potential in hippocampal membranes: implications for receptor function. *Biochim. Biophys. Acta* **1828**, 917–923 (2013).
- Gross, E., Bedlack, R. S. & Loew, L. M. Dual-wavelength ratiometric fluorescence measurement of the membrane dipole potential. *Biophys. J.* **67**, 208–216 (1994).
- Clarke, R. J. & Kane, D. J. Optical detection of membrane dipole potential: avoidance of fluidity and dye-induced effects. *Biochim. Biophys. Acta* **1323**, 223–239 (1997).
- Starke-Peterkovic, T., Turner, N., Else, P. L. & Clarke, R. J. Electric field strength of membrane lipids from vertebrate species: membrane lipid composition and Na<sup>+</sup>-K<sup>+</sup>-ATPase molecular activity. *Am. J. Physiol. Regul. Integr. Comp. Physiol.* **288**, R663–R670 (2005).
- Starke-Peterkovic, T. et al. Cholesterol effect on the dipole potential of lipid membranes. *Biophys. J.* **90**, 4060–4070 (2006).
- Halder, S., Kanaparthi, R. K., Samanta, A. & Chattopadhyay, A. Differential effect of cholesterol and its biosynthetic precursors on membrane dipole potential. *Biophys. J.* **102**, 1561–1569 (2012).
- Bandari, S., Chakraborty, H., Covey, D. F. & Chattopadhyay, A. Membrane dipole potential is sensitive to cholesterol stereospecificity: implications for receptor function. *Chem. Phys. Lipids* **184**, 25–29 (2014).
- Pucadyil, T. J. & Chattopadhyay, A. Role of cholesterol in the function and organization of G-protein coupled receptors. *Prog. Lipid Res.* **45**, 295–333 (2006).
- Paila, Y. D. & Chattopadhyay, A. Membrane cholesterol in the function and organization of G-protein coupled receptors. *Subcell. Biochem.* **51**, 439–466 (2010).

34. Pucadyil, T. J. & Chattopadhyay, A. Cholesterol depletion induces dynamic confinement of the G-protein coupled serotonin<sub>1A</sub> receptor in the plasma membrane of living cells. *Biochim. Biophys. Acta* **1768**, 655–668 (2007).
35. Pucadyil, T. J. & Chattopadhyay, A. Cholesterol modulates ligand binding and G-protein coupling to serotonin<sub>1A</sub> receptors from bovine hippocampus. *Biochim. Biophys. Acta* **1663**, 188–200 (2004).
36. Paila, Y. D., Murty, M. R. V. S., Vairamani, M. & Chattopadhyay, A. Signaling by the human serotonin<sub>1A</sub> receptor is impaired in cellular model of Smith-Lemli-Opitzsyndrome. *Biochim. Biophys. Acta* **1778**, 1508–1516 (2008).
37. Shrivastava, S., Pucadyil, T. J., Paila, Y. D., Ganguly, S. & Chattopadhyay, A. Chronic cholesterol depletion using statin impairs the function and dynamics of human serotonin<sub>1A</sub> receptors. *Biochemistry* **49**, 5426–5435 (2010).
38. Zidovetzki, R. & Levitan, I. Use of cyclodextrins to manipulate plasma membrane cholesterol content: evidence, misconceptions and control strategies. *Biochim. Biophys. Acta* **1768**, 1311–1324 (2007).
39. Mohammad, S. & Parmryd, I. Cholesterol depletion using methyl- $\beta$ -cyclodextrin. *Methods Mol. Biol.* **1232**, 91–102 (2015).
40. Kiss, T. *et al.* Evaluation of the cytotoxicity of  $\beta$ -cyclodextrin derivatives: evidence for the role of cholesterol extraction. *Eur. J. Pharm. Sci.* **40**, 376–380 (2010).
41. Istvan, E. S. & Deisenhofer, J. Structural mechanism for statin inhibition of HMG-CoA reductase. *Science* **292**, 1160–1164 (2001).
42. Sirtori, C. R. The pharmacology of statins. *Pharmacol. Res.* **88**, 3–11 (2014).
43. Schlyer, S. & Horuk, R. I want a new drug: G-protein-coupled receptors in drug development. *Drug Discov. Today* **11**, 481–493 (2006).
44. Zheng, H. *et al.* Palmitoylation and membrane cholesterol stabilize  $\mu$ -opioid receptor homodimerization and G protein coupling. *BMC Cell Biol.* **13**, 6 (2012).
45. Loew, L. M., Scully, S., Simpson, L. & Waggoner, A. S. Evidence for a charge-shift electrochromic mechanism in a probe of membrane potential. *Nature* **281**, 497–499 (1979).
46. Le Goff, G., Vitha, M. F. & Clarke, R. J. Orientational polarisability of lipid membrane surfaces. *Biochim. Biophys. Acta* **1768**, 562–570 (2007).
47. Loew, L. M. Potentiometric dyes: imaging electrical activity of cell membranes. *Pure Appl. Chem.* **68**, 1405–1409 (1996).
48. Robinson, D., Besley, N. A., O’Shea, P. & Hirst, J. D. Di-8-ANEPPS emission spectra in phospholipid/cholesterol membranes: a theoretical study. *J. Phys. Chem. B* **115**, 4160–4167 (2011).
49. Burger, K., Gimpl, G. & Fahrenholz, F. Regulation of receptor function by cholesterol. *Cell. Mol. Life Sci.* **57**, 1577–1592 (2000).
50. Chini, B. & Parenti, M. G-protein-coupled receptors, cholesterol and palmitoylation: facts about fats. *J. Mol. Endocrinol.* **42**, 371–379 (2009).
51. Paila, Y. D., Tiwari, S. & Chattopadhyay, A. Are specific nonannular cholesterol binding sites present in G-protein coupled receptors? *Biochim. Biophys. Acta* **1788**, 295–302 (2009).
52. Oates, J. & Watts, A. Uncovering the intimate relationship between lipids, cholesterol and GPCR activation. *Curr. Opin. Struct. Biol.* **21**, 802–807 (2011).
53. Lee, A. G. Lipid-protein interactions. *Biochem. Soc. Trans.* **39**, 761–766 (2011).
54. Fantini, J. & Barrante, F. J. How cholesterol interacts with membrane proteins: an exploration of cholesterol-binding sites including CRAC, CARC, and tilted domains. *Front. Physiol.* **4**, 1–9 (2013).
55. Jafurulla, M. & Chattopadhyay, A. Membrane lipids in the function of serotonin and adrenergic receptors. *Curr. Med. Chem.* **20**, 47–55 (2013).
56. Paila, Y. D. & Chattopadhyay, A. The function of G-protein coupled receptors and membrane cholesterol: specific or general interaction? *Glycoconj. J.* **26**, 711–720 (2009).
57. Lee, A. G. Biological membranes: the importance of molecular detail. *Trends Biochem. Sci.* **36**, 493–500 (2011).
58. Klein, U., Gimpl, G. & Fahrenholz, F. Alteration of the myometrial plasma membrane cholesterol content with  $\beta$ -cyclodextrin modulates the binding affinity of the oxytocin receptor. *Biochemistry* **34**, 13784–13793 (1995).
59. Bari, M., Battista, N., Fezza, F., Finazzi-Agrò, A. & Maccarrone, M. Lipid rafts control signaling of type-1 cannabinoid receptors in neuronal cells. *Implications for anandamide-induced apoptosis*. *J. Biol. Chem.* **280**, 12212–12220 (2005).
60. Lam, R. S., Nahirney, D. & Duszyk, M. Cholesterol-dependent regulation of adenosine A<sub>2A</sub> receptor-mediated anion secretion in colon epithelial cells. *Exp. Cell Res.* **315**, 3028–3035 (2009).
61. Emery, A. C., Liu, X.-H., Xu, W., Eiden, M. V. & Eiden, L. E. Cyclic adenosine 3',5'-monophosphate elevation and biological signaling through a secretin family G<sub>s</sub>-coupled G protein-coupled receptor are restricted to a single adenylate cyclase isoform. *Mol. Pharmacol.* **87**, 928–935 (2015).
62. Pydi, S. P. *et al.* Cholesterol modulates bitter taste receptor function. *Biochim. Biophys. Acta* **1858**, 2081–2087 (2016).
63. Sjögren, B., Hamblin, M. W. & Svensson, P. Cholesterol depletion reduces serotonin binding and signaling via human 5-HT<sub>7(a)</sub> receptors. *Eur. J. Pharmacol.* **552**, 1–10 (2006).
64. Hu, C.-H. *et al.* Effects of simvastatin and 6-hydroxydopamine on histaminergic H1 receptor binding density in rat brains. *Prog. Neuropsychopharmacol. Biol. Psychiatry* **34**, 1419–1425 (2010).
65. Banfi, C. *et al.* Statins prevent tissue factor induction by protease-activated receptors 1 and 2 in human umbilical vein endothelial cells *in vitro*. *J. Thromb. Haemost.* **9**, 1608–1619 (2011).
66. Ilangumaran, S. & Hoessli, D. C. Effects of cholesterol depletion by cyclodextrin on the sphingolipid microdomains of the plasma membrane. *Biochem. J.* **335**, 433–440 (1998).
67. Kwik, J. *et al.* Membrane cholesterol, lateral mobility, and the phosphatidylinositol 4,5-bisphosphate-dependent organization of cell actin. *Proc. Natl. Acad. Sci. USA* **100**, 13964–13969 (2003).
68. Goodwin, J. S., Drake, K. R., Remmert, C. L. & Kenworthy, A. K. Ras diffusion is sensitive to plasma membrane viscosity. *Biophys. J.* **89**, 1398–1410 (2005).
69. Breusegem, S. Y. *et al.* Acute and chronic changes in cholesterol modulate Na-P<sub>i</sub> cotransport activity in OK cells. *Am. J. Physiol. Renal Physiol* **289**, F154–F165 (2005).
70. Shvartsman, D. E., Gutman, O., Tietz, A. & Henis, Y. I. Cyclodextrins but not compactin inhibit the lateral diffusion of membrane proteins independent of cholesterol. *Traffic* **7**, 917–926 (2006).
71. Cheng, J., Ohsaki, Y., Tauchi-Sato, K., Fujita, A. & Fujimoto, T. Cholesterol depletion induces autophagy. *Biochem. Biophys. Res. Commun.* **351**, 246–252 (2006).
72. Paila, Y. D., Kombrabail, M., Krishnamoorthy, G. & Chattopadhyay, A. Oligomerization of the serotonin<sub>1A</sub> receptor in live cells: a time-resolved fluorescence anisotropy approach. *J. Phys. Chem. B* **115**, 11439–11447 (2011).
73. Mukherjee, S. & Maxfield, F. R. Membrane domains. *Annu. Rev. Cell Dev. Biol.* **20**, 839–866 (2004).
74. Lingwood, D. & Simons, K. Lipid rafts as a membrane-organizing principle. *Science* **327**, 46–50 (2010).
75. Kilsdonk, E. P. C. *et al.* Cellular cholesterol efflux mediated by cyclodextrins. *J. Biol. Chem.* **270**, 17250–17256 (1995).
76. Yancey, P. G. *et al.* Cellular cholesterol efflux mediated by cyclodextrins. Demonstration of kinetic pools and mechanism of efflux. *J. Biol. Chem.* **271**, 16026–16034 (1996).
77. Sanchez, S. A., Gunther, G., Tricerri, M. A. & Gratton, E. Methyl- $\beta$ -cyclodextrins preferentially remove cholesterol from the liquid disordered phase in giant unilamellar vesicles. *J. Membr. Biol.* **241**, 1–10 (2011).
78. López, C. A., de Vries, A. H. & Marrink, S. J. Computational microscopy of cyclodextrin mediated cholesterol extraction from lipid model membranes. *Sci. Rep.* **3**, 2071 (2013).

79. Mohammad, S. & Parmryd, I. Cholesterol homeostasis in T cells. Methyl- $\beta$ -cyclodextrin treatment results in equal loss of cholesterol from Triton X-100 soluble and insoluble fractions. *Biochim. Biophys. Acta* **1778**, 1251–1258 (2008).
80. Liao, J. K. & Laufs, U. Pleiotropic effects of statins. *Annu. Rev. Pharmacol. Toxicol.* **45**, 89–118 (2005).
81. Singh, P., Saxena, R., Srinivas, G., Pande, G. & Chattopadhyay, A. Cholesterol biosynthesis and homeostasis in regulation of the cell cycle. *PLoS One* **8**, e58833 (2013).
82. Starke-Peterkovic, T. & Clarke, R. J. Effect of headgroup on the dipole potential of phospholipid vesicles. *Eur. Biophys. J.* **39**, 103–110 (2009).
83. Duffin, R. L., Garrett, M. P., Flake, K. B., Durrant, J. D. & Busath, D. D. Modulation of lipid bilayer interfacial dipole potential by phloretin, RH421, and 6-ketocholestanol as probed by gramicidin channel conductance. *Langmuir* **19**, 1439–1442 (2003).
84. Clarke, R. J. Dipole-potential-mediated effects on ion pump kinetics. *Biophys. J.* **109**, 1513–1520 (2015).
85. Richens, J. L., Lane, J. S., Bramble, J. P. & O’Shea, P. The electrical interplay between proteins and lipids in membranes. *Biochim. Biophys. Acta* **1848**, 1828–1836 (2015).
86. Cladera, J. & O’Shea, P. Intramembrane molecular dipoles affect the membrane insertion and folding of a model amphiphilic peptide. *Biophys. J.* **74**, 2434–2442 (1998).
87. Chaudhuri, A. & Chattopadhyay, A. Lipid binding specificity of bovine  $\alpha$ -lactalbumin: a multidimensional approach. *Biochim. Biophys. Acta* **1838**, 2078–2086 (2014).
88. Sarkar, P. & Chattopadhyay, A. Micellar dipole potential is sensitive to sphere-to-rod transition. *Chem. Phys. Lipids* **195**, 34–38 (2016).
89. Menge, T., Hartung, H.-P. & Stüve, O. Statins — a cure-all for the brain? *Nat. Rev. Neurosci.* **6**, 325–331 (2005).
90. Keyomarsi, K., Sandoval, L., Band, V. & Pardee, A. B. Synchronization of tumor and normal cells from G1 to multiple cell cycles by lovastatin. *Cancer Res.* **51**, 3602–3609 (1991).
91. Roy, S., Kumar, G. A., Jafurulla, M., Mandal, C. & Chattopadhyay, A. Integrity of the actin cytoskeleton of host macrophages is essential for *Leishmania donovani* infection. *Biochim. Biophys. Acta* **1838**, 2011–2018 (2014).
92. Kalpatnapu, S., Pucadil, T. J., Harikumar, K. G. & Chattopadhyay, A. Ligand binding characteristics of the human serotonin<sub>1A</sub> receptor heterologously expressed in CHO cells. *Biosci. Rep.* **24**, 101–115 (2004).
93. Smith, P. K. et al. Measurement of protein using bicinchoninic acid. *Anal. Biochem.* **150**, 76–85 (1985).
94. Amundson, D. M. & Zhou, M. Fluorometric method for the enzymatic determination of cholesterol. *J. Biochem. Biophys. Methods* **38**, 43–52 (1999).
95. McClare, C. W. F. An accurate and convenient organic phosphorus assay. *Anal. Biochem.* **39**, 527–530 (1971).

## Acknowledgements

This work was supported by the Council of Scientific and Industrial Research, Govt. of India. P.S. thanks the Council of Scientific and Industrial Research for the award of a Shyama Prasad Mukherjee Fellowship. H.C. acknowledges the Council of Scientific and Industrial Research for the award of Senior Research Associateship and the University Grants Commission for UGC-Assistant Professor position. A.C. is an Adjunct Professor of Tata Institute of Fundamental Research (Mumbai), RMIT University (Melbourne, Australia), Indian Institute of Technology (Kanpur), and Indian Institute of Science Education and Research (Mohali). A.C. gratefully acknowledges J.C. Bose Fellowship (Department of Science and Technology, Govt. of India). We thank members of the Chattopadhyay laboratory for their comments and discussions.

## Author Contributions

P.S. and H.C. performed experiments and analyzed data; P.S., H.C., and A.C. designed experiments; P.S. and A.C. wrote the manuscript.

## Additional Information

**Supplementary information** accompanies this paper at doi:[10.1038/s41598-017-04769-4](https://doi.org/10.1038/s41598-017-04769-4)

**Competing Interests:** The authors declare that they have no competing interests.

**Publisher’s note:** Springer Nature remains neutral with regard to jurisdictional claims in published maps and institutional affiliations.



**Open Access** This article is licensed under a Creative Commons Attribution 4.0 International License, which permits use, sharing, adaptation, distribution and reproduction in any medium or format, as long as you give appropriate credit to the original author(s) and the source, provide a link to the Creative Commons license, and indicate if changes were made. The images or other third party material in this article are included in the article’s Creative Commons license, unless indicated otherwise in a credit line to the material. If material is not included in the article’s Creative Commons license and your intended use is not permitted by statutory regulation or exceeds the permitted use, you will need to obtain permission directly from the copyright holder. To view a copy of this license, visit <http://creativecommons.org/licenses/by/4.0/>.

© The Author(s) 2017